Investigating the Effects Methanol-Water Vapor Mixture on a PBI-Based High Temperature PEM Fuel Cell

Samuel Simon Araya[1], Søren Juhl Andreasen, Heidi Venstrup Nielsen, Søren Knudsen Kær

Pontoppidanstræde 101
9220 Aalborg East
Denmark

Abstract

This paper investigates the effects of methanol slip and water vapor in a high temperature proton exchange membrane fuel cell (HT-PEMFC). A H_3PO_4-doped polybenzimidazole (PBI) membrane electrode assembly (MEA), Celtec P2100 of 45 cm^2 of active surface area from BASF was employed. A long-term durability test of around 1250 hours was performed, at various concentrations of methanol-water vapor mixture in the anode feed gas. Vapor concentrations of 5% and 8% by volume in anode feed gas produced a continuous performance decay for as long as they were fed. Impedance measurements followed by equivalent circuit fitting revealed that the effects were most significant for intermediate-high frequency resistances, implying that charge transfer losses were the most significant losses. Vapor mixture of 3% in feed, however, when introduced after operation at 8%, showed positive or no effect on the cell's performance in these tests.

Keywords: High Temperature PEM, Fuel Cell, Methanol, Impedance Spectroscopy

1. Introduction

Methanol is a colorless, neutral, polar and flammable alcohol. There are two ways it can be used in fuel cells, either directly as in a direct methanol fuel cell (DMFC) or by reforming it to hydrogen and carbon dioxide for use in the so called indirect methanol fuel cells, such as HT-PEMFC. In the latter case, the reformer can be implemented on-board the fuel cell system, with an option to even be integrated internally in the fuel cell assembly [1, 2, 3, 4].

The advantages associated with using methanol reformate instead of hydrogen from other sources, such as electrolysis, is mainly the ease of handling of methanol and the possibility of on-site hydrogen production. Contrary to hydrogen, gaseous at room temperature and whose infrastructure and technology implementation would be very costly, methanol being liquid at room temperature is easy to handle, and can use existing gasoline infrastructure with only limited modifications [5, 6]

However, the use of methanol which has the above mentioned advantages, comes at the cost of adding complexity to the fuel cell system. More components are needed, including the reformer itself, the burner and some other auxiliaries. Moreover, reforming by products namely, CO and CO_2 have undesirable effects on the fuel cell's performance and health. While CO_2 mainly dilutes the reactants, CO is known to preferentially adsorb on the Pt surface, thereby taking up active catalyst sites and degrading the performance of the cell [7, 8, 9, 10]. HT-PEMFCs have come a long way in increasing the tolerance to CO. Das et al. [11] found that CO concentration up to 5% could be tolerated without any fuel cell performance losses, at 180°C, < 0.3 A/cm^2 and > 0.5 V. This is mainly due to reduced CO adsorption and the removal of adsorbed CO via oxidation at higher temperatures [12, 13]. Nevertheless, CO poisoning remains one of the limiting factors of the lifetime of HT-PEMFCs, and hence, crucial for their commercialization.

Presently, methanol production heavily rely on syngas produced from coal and natural gas, both of which are fossil fuels. Since the reforming process also produces CO_2, the use of methanol in fuel cells is not completely CO_2 neutral. For this to happen, methanol for fuel cell application should be produced from renewable sources, an issue that is common to all sources

of hydrogen. However, methanol can be produced in big quantities from renewables of various biomass sources such as wood, forest waste, peat, municipal solid wastes, sewage and even chemical recycling of CO_2 from the atmosphere [14, 15]. Solid oxide electrolyzer for-example, can be used to produce synthesis gas, a mixture of CO and hydrogen, from CO_2 and steam at high temperature that can then easily be converted into methanol or dimethyl ether (DME) [16]. This makes methanol, at the current stage and with currently available technology, the most practical proposition for fuel cells of a greener future.

Even though, the conversion of methanol in a reformer never goes to 100%, the possible poisoning effects of unconverted methanol are rarely studied in HT-PEMFCs. Methanol crossover with subsequent oxidation in the cathode and methanol dehydrogenation on Pt-surface of both electrodes, with intermediate formation of CO are some of the degrading mechanisms in DMFCs [5, 17, 18]. Similar mechanisms may be expected to be at play in a PBI based HT-PEMFC as well, but the quantities of methanol involved are much smaller in this case, which makes experimental characterization more complex. Methanol dehydrogenation on Pt surface is a fairly well studied phenomenon, especially in DMFCs [17, 18, 19]. However, the intermediates of the process and the different pathways that take place at various potentials are not well defined. Adsorbed CO is usually identified as the main stable surface product, which as mentioned before has a poisoning effect on Pt catalyst. The different pathways depend on the electrode potential and the surface structure of Pt electro-catalyst, and at higher electrode potentials non-CO pathways are also observed [18]. Other intermediates include CO_2, formaldehyde and formic acid [18, 20]. Unlike the effects of CO and CO_2, which are fairly well studied, it is not clear how the rest of the complex intermediates affect the fuel cell.

This work investigates experimentally the effects of methanol slip in a H_3PO_4/PBI-based HT-PEMFC, to broaden the understanding of the effects of a reformate gases by adding methanol-water vapor mixture to the array of poisoning impurities. The analysis is made based on impedance measurements done over a period of time, which were then fitted to an equivalent circuit model. Literature review on PEMFCs, HT-PEMFCs and DM-FCs, together with the observed trends were used to analyse the different degradation mechanisms.

2. Experimental

Figure 1 illustrates schematically the experimental setup used in this study. It consists of a LabView® based fuel cell control system and a Gamry FC350 hardware and control software for impedance measurements. Mass flow controllers were used for H_2 and air, and a vapor delivery system composed of a dosing pump and an electrically heated evaporator was used for the delivery of methanol-water vapor mixture. The fuel cell used is a unit cell assembly of a 45 cm^2 active area with a Celtec® P-2100 MEA from BASF, sandwiched between graphite composite flow plates of serpentine flow channels.

The fuel cell was subjected to a break-in procedure for more than 100 hours before methanol was added to the anode feed gas. Operating conditions for break in were set at: current density of 0.2 A/cm^2 (9A), temperature of 160 °C, stoichiometric ratio of hydrogen, λ_{H_2}=1.2 and that of air , λ_{Air}=4.

Since to the knowledge of the authors, this is the first study of its kind, the scope of the work was limited to generally investigate the effects of methanol-water vapor mixture on an operating HT-PEMFC. For this, it was decided to vary their composition in the feed gas, and start at a rather high concentration of vapor mixture of 5% by volume followed by 8% in order to accelerate the tests. Furthermore, to check the reversibility of the effects of the vapor mixture, the concentrations were reduced to 3% by volume before their supply was completely interrupted for operation on pure hydrogen. The fuel cell was then restarted at the end of tests for further reversibility check. It is worth noting, therefore, that varying the methanol-water vapor concentration frequently may limit the generalization results, while still giving invaluable qualitative insight into the changes in the fuel cell performance.

The tested methanol concentrations are above what can be expected from the current technology of reforming processors, which depending on operation temperature and feed rates, can give a hydrogen yield that can keep unconverted methanol-water vapor mixture to lower percentages [21, 1]. This can however increase in the case of stack operation, as there may be some accumulations over time, and also possible condensation during shut down. Therefore, the reason for undertaking tests at such high methanol concentrations is not only to accelerate the durability tests, but also investigate the worst operation conditions that may occur during stack operation.

Temperature and current density were kept constant at 160 °C and 0.22 A/cm^2 (10 A), respectively, through-
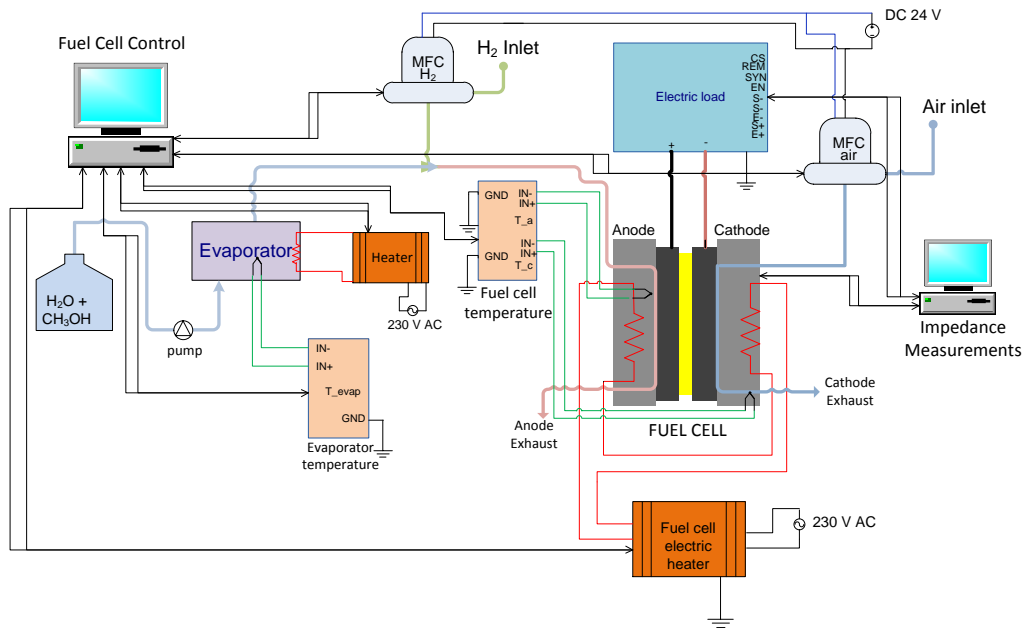
Figure 1: Experimental setup.

out the duration of the experiments. For methanol-water vapor mixture a steam to carbon ratio of 1 is assumed for the entire experiment.

Impedance measurements were done at frequency sweeps between 10 kHz and 1 Hz. For the analysis and interpretation of impedance data, an equivalent circuit (EC) model shown in Fig. 2 was chosen from literature [22]. It is composed of ideal circuit elements, where R_{ohmic}, corresponds to the ohmic losses of the cell, which are mainly due to the electrolyte resistance and contact resistances between interfaces. R_{hf} and R_{if}, are charge transfer resistances between electrode and electrolyte interfaces for high frequency range and intermediate frequency range, respectively. The last resistance, R_{lf}, is the low frequency resistance, which is usually related to mass transport process (finite diffusion). The choice of the model was based on the number of time constants observed on the the measured impedance data. Three time constants were observed, which are represented by the three R/CPE loops in Fig. 2.

3. Results and Discussion

3.1. Overall durability

A durability test of the duration of 1250 hours was performed, in which the content of methanol-water va-

por in the anode feed was varied. It is observed that the degradation rate for operation on pure hydrogen taken over a period of 123 hours gives a near horizontal line on the voltage-time plane (Fig. 3). The voltage drop rate is calculated to be -20 μV/h on average in this period. Moçotéguy et al. [10] found a voltage drop rate of the same order of magnitude of -41 μV/h over a period of 505 hours on a Celtec-P1000 MEA, at a current density of 0.4 A/cm^2 and temperature of 160 °C. Schmidt and Baurmeister [23] also did long-term durability studies on HT-PEMC based on the same MEA and found voltage drop rate of -5 μV/h over a period of 3000 and 6000 hours, respectively, which is also the degradation rate claimed by BASF for the MEA. The conditions for their tests were similar to ours, with cell temperature kept at 160 °C and current density at 0.2 A/cm^2.

In comparison, operation in the presence of 5% by volume of methanol-water vapor mixture in the anode feed gas shows a degradation rate of -900 μV/h, which is evidently deviated from the case of a pure hydrogen operation. Li et al. [24] worked with reformate in their long-term durability tests with a voltage drop rate of -20 μV/h, which however can not be directly compared with the current work as they used natural gas reformate.

Further increase in methanol content to 8% produces even steeper degradation slope. The rate in this case is
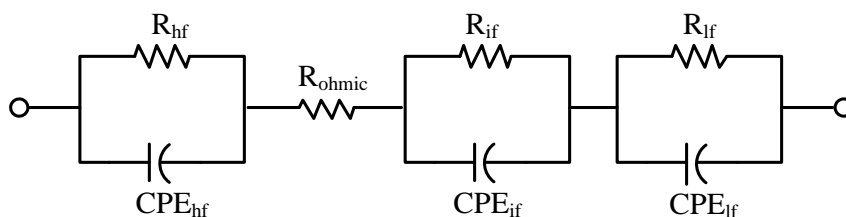
3

Figure 2: Equivalent circuit model for fitting with measured impedance data.

-3.4 mV/h and degradation continued without any sign of stabilization until the methanol content in the feed gas was reduced. The concentration was reduced to 3% by volume and this caused a rapid recovery in the beginning, which then continued slowly until the supply was shut down. The total recovery was a modest 0.03 V over 157 hours with respect to a total voltage drop of 0.17 V, caused by the vapor mixture until that point over a period of 988 hours. When the methanol supply was interrupted, further recovery of the fuel cell performance followed by slow degradation was observed. The fuel cell was restarted before end of tests and a significant rise in voltage was noticed, 11% increase in cell voltage.

It appears clear that, high concentrations of methanol have a degrading effects on the performance of the fuel cell. However, lower concentrations of methanol below 3% did not show any degrading effects for the duration in which they were tested. The recovery in cell performance seen at later stages of the test, including the restart of the fuel cell, suggests that some of the effects of methanol-water vapor mixture are reversible.

3.2. Overall EIS

To be able to understand and attribute the different losses to the different frequency regions, a detailed EIS analysis was performed. Here below, a summary of the overall observation on the impedance spectra before the data is fitted to equivalent circuit model, and a successive analysis of the fitted results is given.

In Fig. 4 it can be seen from the Nyquist plot that the impedance spectra expands with time and with the introduction of the methanol-water vapor mixture, while also being displaced to the right on the real axis. The bode diagram also shows that the maximum phase shift and the frequency at which it occurs increases with time. Similar trend of expanding spectra is seen in [25] with decrease in temperature of a HT-PEMFC, and is a typical indication of increased losses manifested by increased impedance.

Contrary to expectations, the spectra in Fig. 4 do not show any inductive behavior at high frequency. High frequency inductive behavior is usually present in impedance measurements due to the wiring and other instrumental non-idealities [26, 25]. In the current work the recommended wiring supplied by Gamry was used to connect the impedance measurement system to the fuel cell, and other wires were used for the rest of the setup. Mamlouk and Scott [25] limit the inductive behavior to above 10 kHz. Otomo et al. [27] on the other hand did not see a high frequency inductive behavior in their sweep of until more than 10 kHz, but observed instead, a low frequency inductive loop for methanol electro-oxidation in the anode. Despite these uncertainties and a relatively high positive $-Z_{img}$ values, the changes in impedance observed due to variation in the concentration of methanol-water vapor mixture are rather typical of performance degradation, and follow closely the overall durability plot in Fig. 3.

It can also be noticed that, a high frequency loop is only seen on measurements before the tests with methanol started, after which instead a low frequency semicircle evolves increasingly with time and with increase in methanol concentration. Moçotéguy et al. [10] also observed that the high frequency loop disappears with increase in degradation, which makes it plausible to suggest that the disappearance of this loop is related to increased degradation from poisoning due to methanol.

In the beginning, as methanol-water vapor mixture was introduced to the system the impedance spectrum shrinks, as can be seen in Fig. 4. This shrinking of spectrum could imply that the vapor mixture has an initial positive impact on the cell's performance. This may be attributable to the presence of water vapor, which enhances the cell performance by promoting the proton conduction through the membrane [28]. However, wa-
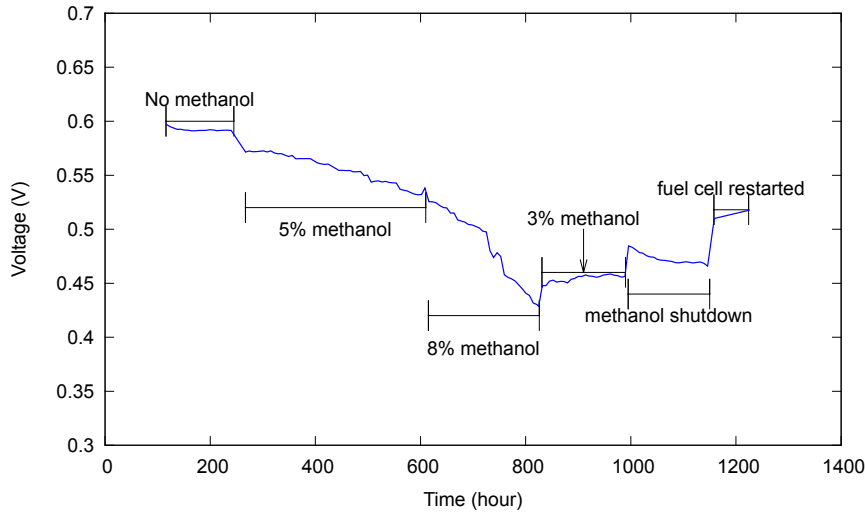
4

Figure 3: Cell voltage during the entire period of experiments.

ter is also reported to have a degrading effect by leaching of H_3PO_4 (PA) from the PBI membrane at lower temperatures during fuel cell shut down [29]. This is expected to be limited in the current work, as there were no start/stop cycles tested, in which dilution of acid at lower temperature during shut down is suggested [30].

Further continuous operation at 5% and then successively at 8% causes the impedance spectra to continuously expand. This expansion implies loss in cell performance with time, according to the increase in methanol concentration. The increase in spectra size stops for operation at 3% of vapor mixture and restarts slowly when the methanol supply is interrupted, suggesting that poisoning effects are seen only at high concentrations of methanol.

At the same time, it is observed that more methanol in anode feed means more pronounced low frequency loops. In fact, the shapes of the spectra before methanol was introduced and after methanol supply was interrupted resemble each other in the low frequency region, in that, they have less pronounced low frequency loops. Otomo et al. [27] observed an inductive loop at frequencies lower than 0.1 Hz. They concluded that since the inductive loop appeared through the electro-oxidation, it was an indication of the fact that during the electro-oxidation of methanol the passage from the intermediates to the products was the rate-determining process of the overall reaction. The low frequency loop in our case could be characterized by the start of such behavior, or just mass transport and diffusive limitations. In either case it can be said that, methanol-water vapor mixture

increases the losses in this frequency range. Ji et al. [5] reported that the hydroxyl groups of methanol forming hydrogen bonds, are more likely to accept hydrogen atoms than to donate hydrogen atoms. This may slow down diffusion of hydrogen in the anode side, implying that diffusion losses are not limited to the cathode side alone.

3.2.1. Overall fitted resistances

In the following, the different resistances are analysed individually and an overview of their trend is shown in Fig. 5.

Ohmic resistance

Generally speaking, there is not significant change in ohmic resistance. There is a slight decrease in R_{ohmic} at all the stages of the tests, but it is cancelled out by the increase seen at each change of methanol content in feed gas. Assuming that, R_{ohmic} represents the contact resistances and electrolyte resistance, it can be said methanol-water vapor mixture has negligible effect on the overall conductivity of the electrolyte. The slight decrease in R_{ohmic} observed in all the stages of the tests, may be attributed to the presence of water vapor, which enhances the proton conduction in PBI-based polymer electrolytes [28]. Membrane thinning due to degradation may also be another contributor to such an effect.

On the contrary, the vapor mixture has also the effect leaching H_3PO_4 from the PBI membrane, which being the proton conduction media may lead to performance degradation [29]. Moçotéguy et al. [10] observed
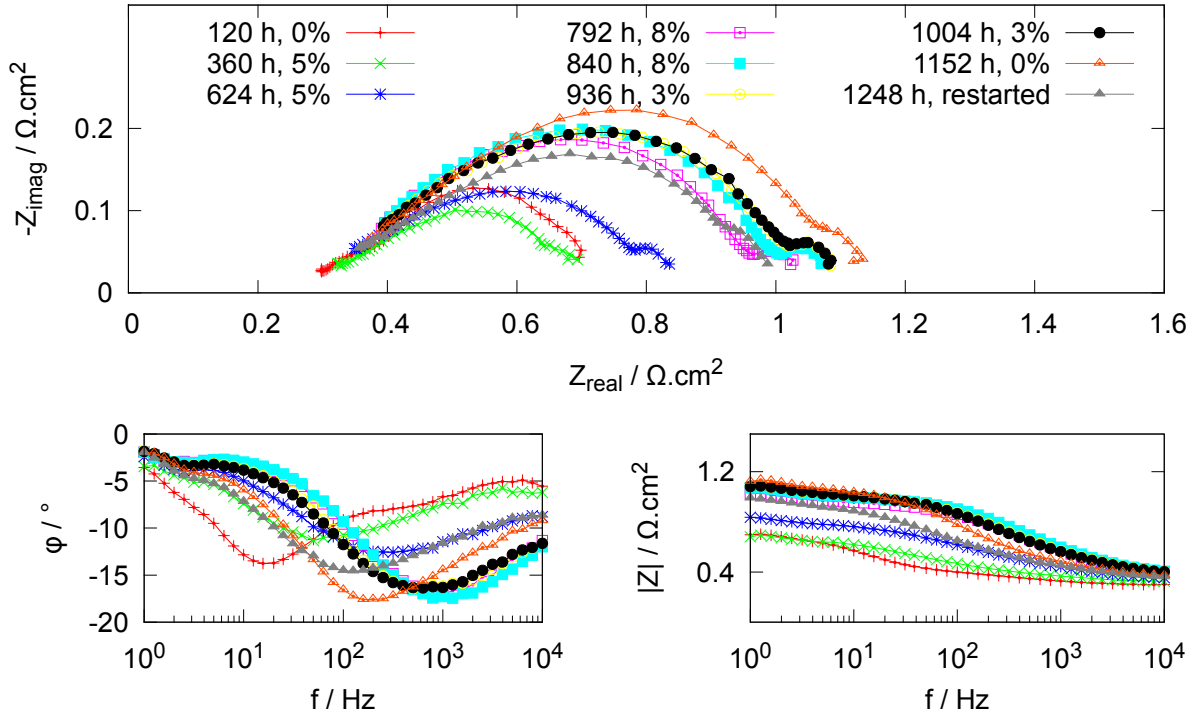
Figure 4: Nyquist and bode plots comparing the impedance spectra at different conditions, with the percentages indicating the methanol-water vapor content in the anode feed gas.

PA leaching without significant changes in ohmic resistance in their long-term durability tests. They however tested start/stop cycling every 12 hours, in which PA leaching may be accelerated by liquid water formed at lower temperatures during fuel cell shut down. In our case, start/stop cycling were not tested, and therefore PA leaching may be very limited.

High frequency resistance

There is a clear increase in high frequency resistance in the presence of 5% methanol as can be seen in Fig.5. The increase is strangely arrested when the methanol content is raised to 8%, and then slightly increases on the passage to and during operation at 3%, where it then remains constant towards the end. Lastly, when methanol-water vapor supply was interrupted the effects reversed partially and remained constant even after the fuel cell was restarted.

Thus, it appears that, it is more the change in vapor content of the feed gas that determines the magnitude of R_{hf} than the vapor content itself. This is seen from the fact that R_{hf} increases every time the amount of vapor is changed, and then stabilizes. A possible explanation for

this could be that, some saturation or equilibrium condition is established at the interface after each change in concentration. This however, can not be said with certainty from impedance analysis alone.

Intermediate frequency resistance

In the intermediate frequency range, a slow and progressive increase in resistance is seen during operation with 5% methanol. The increase is then more pronounced for 8% and continues to increase until the methanol content is reduced to 3%, where R_{if} remains constant. It is as if operation on 3% methanol by volume stops the increase in R_{if}, which resumes when methanol supply is interrupted. This trend continues at different rates until the fuel cell is restarted. This could mean that there were some life time issues that were masked by equilibrium condition at 3% operation but were later revealed when this was disrupted by methanol shut down. It seems however, they are reversible durability issues from which the fuel cell recovered fast when restarted.

Although, the intermediate frequency region is usually associated with charge transfer limitation of cathodic oxygen reduction reaction (ORR) [31], some pro-
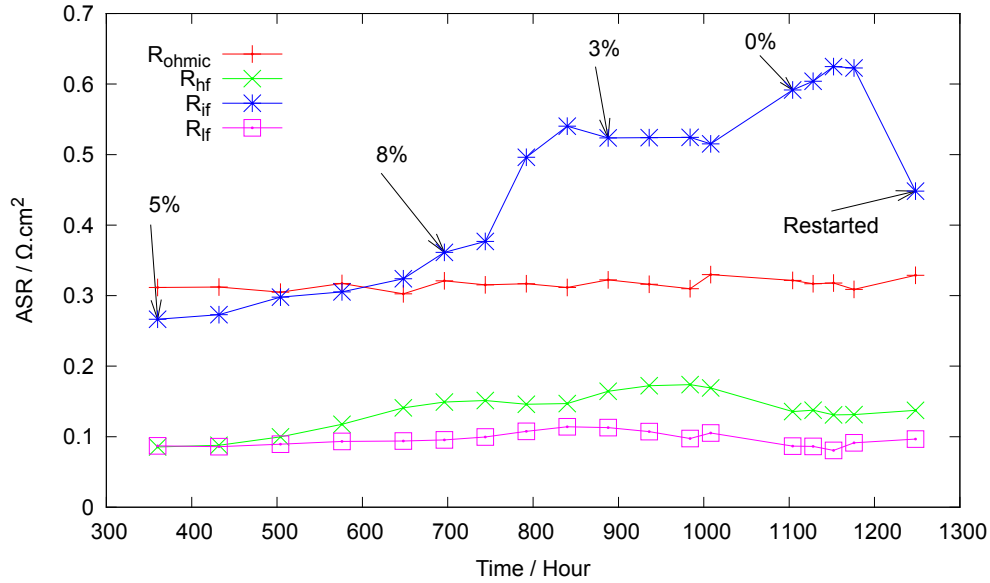
6

Figure 5: Variation of all the resistances in time and with varying methanol content. The starting points of the different stages of the experiment are marked on R_{if}.

cesses in the anode side may also contribute to part of these resistances.

It is also interesting to notice that, R_{if} follows closely the trend of the durability profile in Fig. 3, and therefore, can be a useful parameter for fuel cell diagnosis. That is, the increase in R_{if} corresponds to increased voltage drop due to catalyst degradation and can be a good indication of the state of health of the fuel cell.

Low frequency resistance

Similarly to the R_{if}, the low frequency resistance R_{lf} showed a successive increase for 5% and 8% methanol-water vapor mixture, proportionally to the vapor content. Unlike in the former case however, an initial decrease followed by slight increase was observed both during operation with 3% vapor mixture and when the supply of vapor was interrupted. The low frequency loop is usually characterized by diffusion limitations in the gas diffusion layer (GDL) [32], which may results in the same limitations on the catalyst surface as well. This could imply, that higher contents of vapor mixture increases these diffusion losses, while small amount of vapor may promote the diffusion of the gaseous species both on the GDL and the catalyst layer.

3.3. Impedance evolution for each methanol concentration

In the following, the effects of different methanol concentrations in the anode feed gas are analysed according to the chronological order in which they were varied during the experiments.

3.3.1. 5% methanol-water vapor mixture

As a typical sign of performance decay, the impedance spectra increases in size as the cell runs on 5% methanol-water vapor mixture. In Fig.6(a) it can be seen how the marked characteristic frequencies are displaced more to the right with respect to each other, showing a more sluggish electrical behaviour. While ohmic resistances remain almost unaltered throughout the experiments, there is a clear general increase for all other resistances, proportionally to the methanol content of the feed gas .

In particular, the changes are most visible for high and intermediate frequency, an overall increase of 75% and 25% , respectively. The low frequency loop, which represents finite diffusion, although moves more the right, only slightly increases in size. This is seen in Fig.6(e), where the increase is not significant, accounting only to an overall increase of 9%.
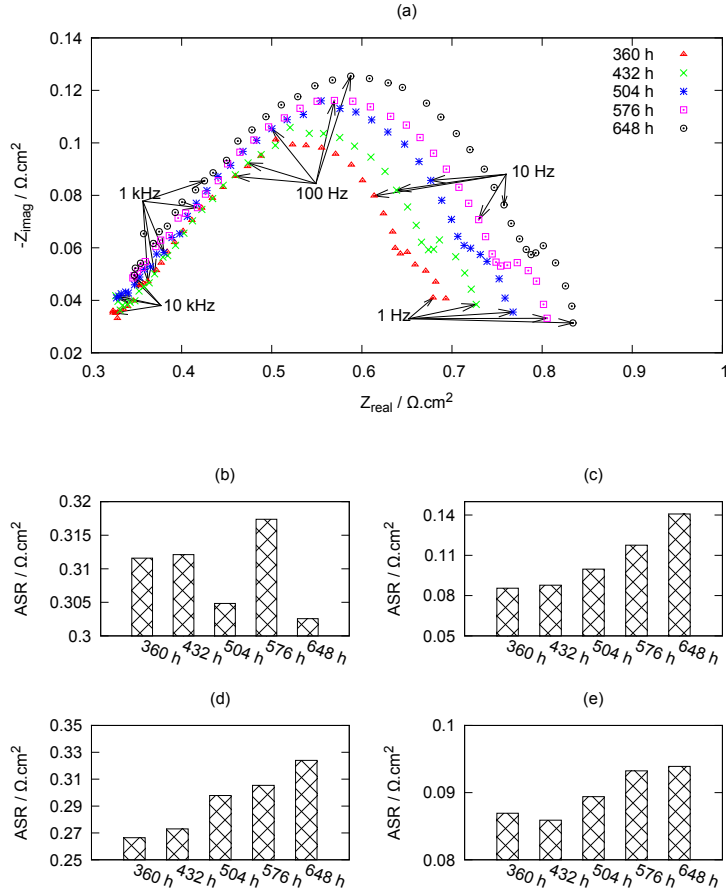
7

Figure 6: Impedance analysis of operation at 5% methanol-water vapor mixture (a) evolution of the impedance spectra in time (b) ohmic resistance (c) high frequency resistance (d) intermediate frequency resistance (e) low frequency resistance.

3.3.2. 8% methanol-water vapor mixture

In this case the spectra continues to increase in size and the characteristic frequencies continue to move to right. It can be noticed in Fig. 7(a) that the relaxation frequency of the intermediate loop is now more than 100 Hz.

In Fig. 7(b), a small general decrease in R_{ohmic} is noticed, while in Fig. 7(c) R_{hf} stabilizes at the last values of operation with 5% methanol with a very slight decrease at the end. The increase in resistances is most important for intermediate and low frequency ranges in this case, Fig. 7(d) and (e), respectively. This implies that charge transfer and diffusion limitations are both affected by such high concentration of vapor misture in the anode feed.

Consequently, the usual assumption that the intermediate frequency region is associated with ORR limitations on the cathode side [31], would suggest that there may be vapor cross-over at this high level of methanol concentration. The methanol may then electro-oxidize by dehydrogenation on the Pt catalyst on the cathode side, which may in turn limit the diffusion of oxygen on the catalyst surface. While this is a typical situation in a DMFC [5, 17, 18], it may not be the only explanation in the case of an HT-PEMFC. Some of the anode processes, possibly the complex intermediates of methanol electro-oxidation, such as formaldehyde that also contain oxygen, may be contributing to the intermediate frequency resistances.

However, vapor cross-over is still reasonably one of the degrading mechanisms, as the PBI membrane that is normally employed, is characterized by high permeability to water vapor [28]. Li et al. [12] reported that methanol also shows similar modes of permeation as that of water through a PBI membrane, mainly via diffusion. Daletou et al. [28] found that water vapor interacts
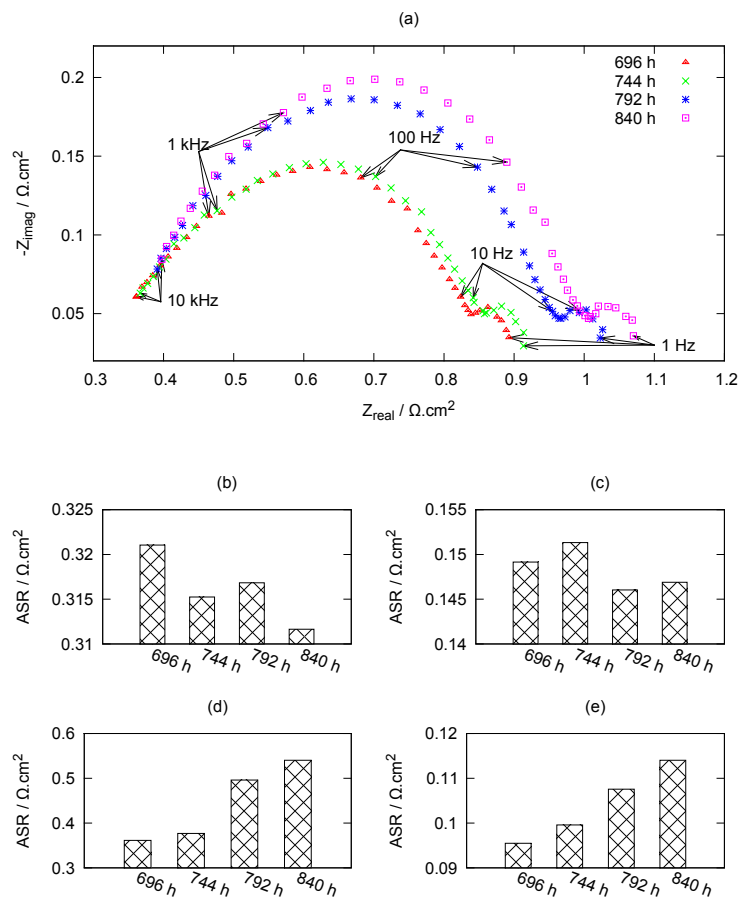
Figure 7: Impedance analysis of operation at 8% methanol-water vapor mixture (a) evolution of the impedance spectra in time (b) ohmic resistance (c) high frequency resistance (d) intermediate frequency resistance (e) low frequency resistance.

strongly with the PBI and attributed its relatively high permeation rate to its solubility in H_3PO_4 and its interaction with PBI. If methanol also has similar level of interactions with PBI, it can be expected that it permeates and electro-oxidized on the catalyst layer.

3.3.3. 3% methanol-water vapor mixture

Reduction of vapor mixture concentration to 3%, visibly freezes the Nyquist diagram in Fig. 8(a). However, a closer look at the fitted resistance values of the proposed equivalent circuit model reveals some changes. A slow decrease is observed for both R_{ohmic} and R_{lf}, while R_{hf} on the other hand shows a slow increase. R_{if} remains almost unaltered for most of the 3% ran. Anomalous shift of trend is seen for the last measurement. However, instrumental and fitting uncertainties apart, it can be said that charge transfer losses, though moderate, they contribute to most of the losses at operation with 3% vapor.

Evidently, measurements taken during operation at 3% of vapor mixture in the anode feed are the most significant, as current reforming technologies can limit the unconverted methanol in the reformate gas to even lower amount by volume. However, as this concentration was applied after the fuel cell has been operating at even higher vapor concentrations for accelerated tests, results may not be directly generalized. That is, if 3% vapor mixture is introduced after operation on pure hydrogen, the effects may differ. Nevertheless, for what concerns the current work, it can be said that the effects of methanol at such concentrations and lower are negligible from a performance point of view. This is seen from the fact that R_{if} in Fig. 8(d), which indicates more directly the performance by following the voltage drop, remains almost constant. Enhancements in other regions of the frequency sweep or other processes are also seen, as R_{ohmic} and R_{lf} decrease in time. They represent the electrolyte resistance and finite diffusion limitations, respectively, and they show a generally linearly decreasing trend, by almost the same magnitudes.

3.3.4. No vapor supply

Contrary to what would be expected, the impedance continued to increase when methanol supply was interrupted. The characteristic frequencies return to the placements similar to that of the initial stages of the experiment, and the finite diffusion loops at low frequency range become less pronounced.

Fitted equivalent circuit resistances suggest that there is a slow decrease in resistance at all frequency regions, except at the intermediate one, which shows a slow and quasi linear increase instead. This manifests the continued increase in impedance, which may be attributed to the fact that the fuel cell was already aged and that without refresh cycles no recovery could be achieved. In fact, when the fuel cell was restarted as one of the suggested refresh cycles, it recovered part of its performance sharply. This is seen from the fact that the impedance spectrum shrinks in Fig. 9(a), which results in sharp drop in R_{if} in Fig. 9(d).

3.4. Post-mortem analysis of the MEA

At the end of the impedance tests, the fuel cell was disassembled and a scanning electron microscopy (SEM) was performed on the MEA. This was then compared with an SEM imaging and atomic distributions of unused MEA of the same type, Celtec P-2100 from BASF.

Typical SEM images, and plots for Pt distribution and PA levels along the cross-section of a new MEA and the one used in this work are given in Fig. 10 and Fig. 11, respectively. PA levels and Pt distribution are similar in both cases. There is only displacement of the peaks, possibly due to the swelling caused by the intake of the different species in the anode feed. Indeed, PA leaching is suggested to have effects at lower temperatures of fuel cell shut down [29]. This was not the case in this work as there were no intentional start/stop cycles tested. This may have limited the PA leaching and its effects on the fuel cell.

A slightly higher concentration of Pt is seen on some points of one side of the used MEA with respect to the unused one. As can be noticed also from the SEM micrography, this could be a manifestation of a slight Pt agglomeration. On most points however, both PA level and Pt concentrations remain almost unaltered and therefore their relation to the presence of methanol-water vapor could be said limited .

4. Conclusion

This report gives a general insight into the effects of methanol-water vapor miture in an HT-PEMFC, by means of accelerated tests. Degradation rate for operation with pure hydrogen was found to be -20 μV/h over the first 123 hours after break-in, which is in the same order of magnitude as in the literature. Degradation rates in the presence methanol-water vapor mixture were higher, -900 μ/V for 5% and -3.4 mV/h for 8%. Both from durability curves and impedance analysis it is seen that continuous operation with 5% or 8% of vapor mixture degrades the fuel cell severely. Methanol dehydrogenation on Pt surface with formation of CO and
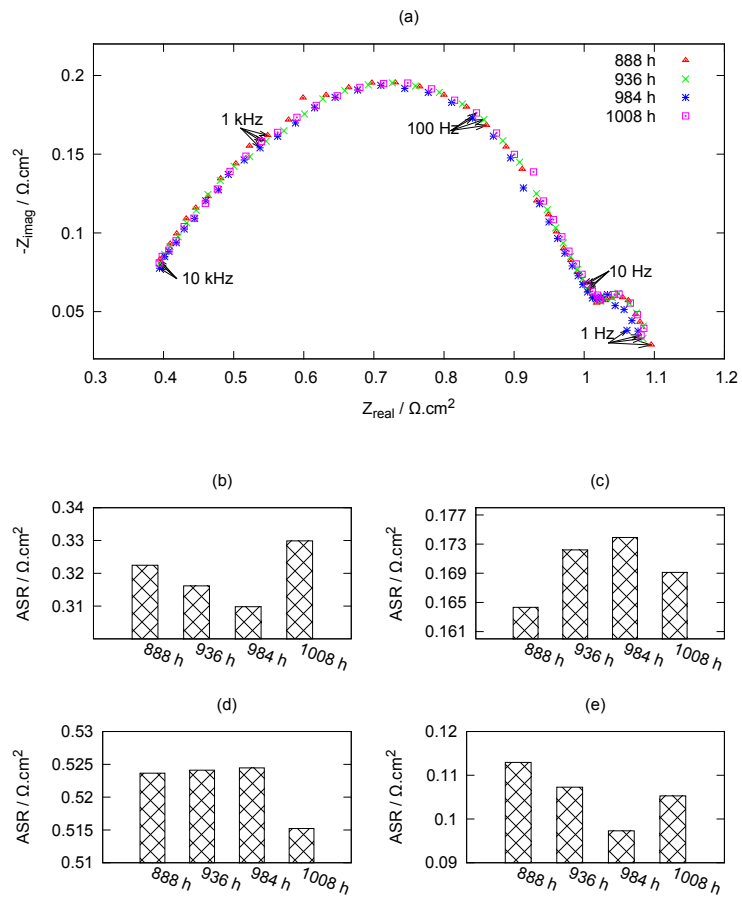
Figure 8: Impedance analysis of operation at 3% methanol-water vapor mixture (a) evolution of the impedance spectra in time (b) ohmic resistance (c) high frequency resistance (d) intermediate frequency resistance (e) low frequency resistance.
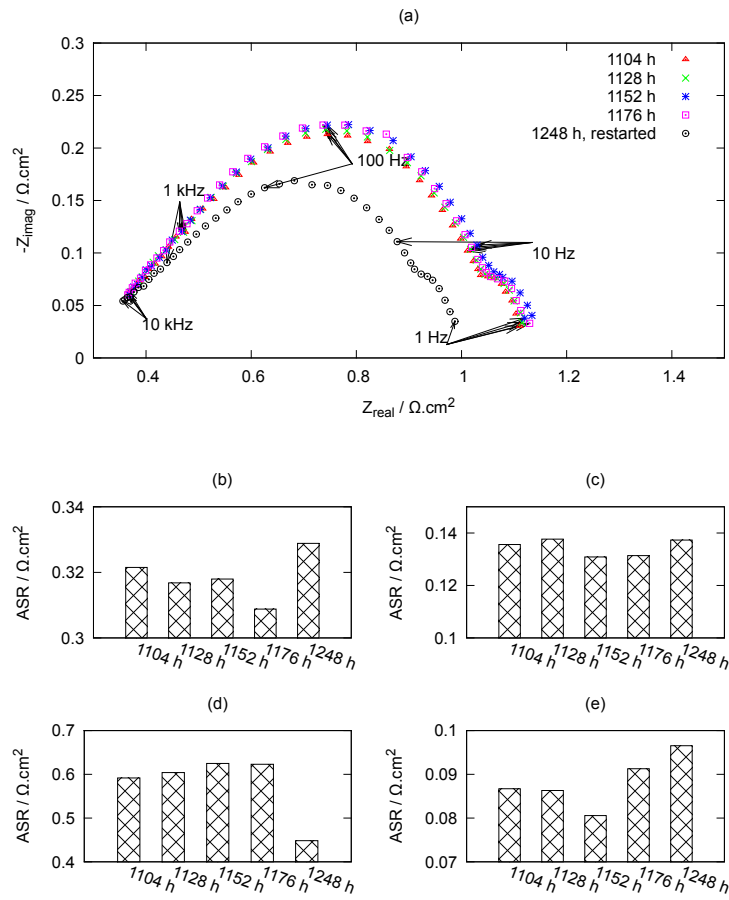
Figure 9: Impedance analysis of operation with no methanol-water vapor mixture, where in the last measurement the fuel cell has been restarted (a) evolution of the impedance spectra in time (b) ohmic resistance (c) high frequency resistance (d) intermediate frequency resistance (e) low frequency resistance.
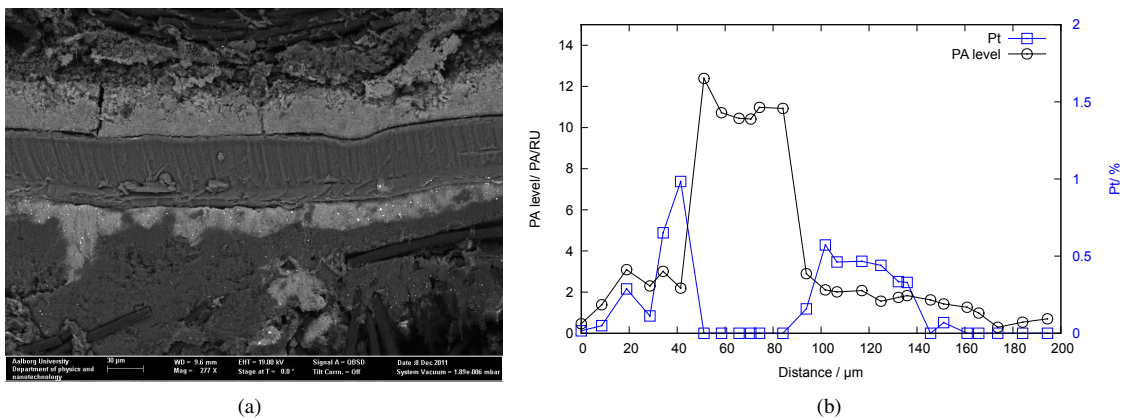

Figure 10: SEM analysis of the crossection of a new Celtec P-2100 MEA (a) SEM micrography (b) Pt and PA level distribution.
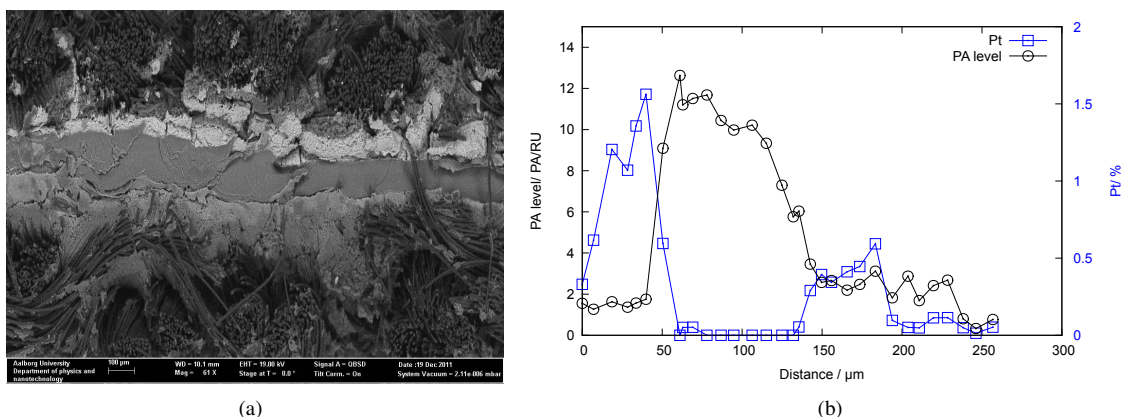
Figure 11: SEM analysis of the crossection of the Celtec P-2100 MEA used in the current work (a) SEM micrography (b) Pt and PA level distribution.

other complex intermediates, that then poison the catalyst can be suggested as a degrading mechanism. However, more tests and comparisons with other characterization techniques are needed to identify the exact mechanism by which methanol degrades the performance of an HT-PEMFC.

In conclusion, it can be said that while high concentrations of vapor mixtures (5 and 8% of vapor) in the anode feed clearly degrade the performance of the fuel cell, lower concentrations below 3% of vapor mixture, which are more significant to real world operation have negligible effect in this work. It is worth noting that that lower concentrations were tested after higher concentration, and caused a partial recovery in the cell's performance, signifying that the effect of the vapor miture are in part reversible. PA leaching does not seem be an issue, but the cells performance should be tested under start/stop cycling stress to reveal whether the vapor could result in PA leaching at lower temperatures. Even though time consuming, future works should also address durability tests based on single concentration of around 2% vapor mixture for the entire lifetime of a fuel cell. If this is done by relating various characterization techniques with each other, it would give generalizable results on the degradation mechanisms.

References

[1] Pan C, He R, Li Q, Jensen JO, Bjerrum NJ, Hjulmand HA, et al. Integration of high temperature PEM fuel cells with a methanol reformer. J Power Sources 2005;145(2):392 –8. Selected papers presented at the Fuel Cells Science and Technology Meeting.

[2] Ouzounidou M, Ipsakis D, Voutetakis S, Papadopoulou S, Seferlis P. A combined methanol autothermal steam reforming and PEM fuel cell pilot plant unit: Experimental and simulation studies. Energy 2009;34(10):1733 –43. 11th Conference on Process Integration, Modelling and Optimisation for Energy Saving and Pollution Reduction.

[3] Park DE, Kim T, Kwon S, Kim CK, Yoon E. Micromachined methanol steam reforming system as a hydrogen supplier for portable proton exchange membrane fuel cells. Sensors and Actuators A: Physical 2007;135(1):58–66. doi: 10.1016/j.sna.2006.07.008.

[4] Avgouropoulos G, Papavasiliou J, Daletou MK, Kallitsis JK, Ioannides T, Neophytides S. Reforming methanol to electricity in a high temperature PEM fuel cell. Appl Catal B 2009;90(34):628 –32.

[5] Ji X, Yan L, Zhu S, Zhang L, Lu W. Methanol Distribution and Electroosmotic Drag in Hydrated Poly (perfluorosulfonic) Acid Membrane. The Journal of Physical Chemistry B 2008;112(49):15616–27. doi:10.1021/jp8066469.

[6] Ogden JM, Steinbugler MM, Kreutz TG. A comparison of hydrogen, methanol and gasoline as fuels for fuel cell vehicles: implications for vehicle design and infrastructure development. Journal of Power Sources 1999;79(2):143 –68. doi:DOI: 10.1016/S0378-7753(99)00057-9.

[7] Yan WM, Chu HS, Lu MX, Weng FB, Jung GB, Lee CY. Degradation of proton exchange membrane fuel cells due to CO and CO_2 poisoning. J Power Sources 2009;188(1):141 –7.

[8] Du B, Pollard R, Elter JF, Ramani M. Performance and Durability of a Polymer Electrolyte Fuel Cell Operating with Reformate: Effects of CO, CO_2, and Other Trace Impurities. Springer New York. ISBN 978-0-387-85536-3; 2009, p. 341–66.

[9] Tang Y, Zhang H, Zhong H, Xu Z. In-situ investigation on the CO tolerance of carbon supported Pd¢Pt electrocatalysts with low Pt content by electrochemical impedance spectroscopy. International Journal of Hydrogen Energy 2012;37(3):2129–36. doi:10.1016/j.ijhydene.2011.10.104.

[10] Moçotéguy P, Ludwig B, Scholta J, Barrera R, Ginocchio S. Long Term Testing in Continuous Mode of HT-PEMFC Based H 3 PO 4 /PBI Celtec-P MEAs for μ-CHP Applications. Fuel Cells 2009;9(4):325–48. doi:10.1002/fuce.200800134.

[11] Das SK, Reis A, Berry K. Experimental evaluation of CO poisoning on the performance of a high temperature proton exchange membrane fuel cell. J Power Sources 2009;193(2):691 –8.

[12] Li Q, He R, Jensen J. PBI¢Based Polymer Membranes for High Temperature Fuel Cells ¢ Preparation, Characterization and Fuel Cell Demonstration. Fuel Cells 2004;4(3):147–59. doi: 10.1002/fuce.200400020.

[13] Modestov A, Tarasevich M, Filimonov V, Davydova E. Co tolerance and co oxidation at pt and ptru anode catalysts in fuel cell with polybenzimidazoleh3po4 membrane. Electrochimica Acta 2010;55(20):6073 –80. doi:10.1016/j.electacta.2010.05.068.

[14] Bromberg L, Cheng WK. Methanol as an Alternative Transportation Fuel in the U.S.: Options for Sustainable and/or Energy-Secure Transportation. Tech. Rep.; Massachusetts Institute of Technology, Sloan Laboratories for Automotive and Aircraft Engines Cambridge, MA 02139 USA Battelle Columbus, OH USA; 2010-11.

[15] Olah GA, Goeppert A, Prakash GKS. Beyond Oil and Gas: The Methanol Economy. Wiley; September 2009.

[16] Hauch A. Solid Oxide Electrolysis Cells ¢ Performance and Durability; vol. 37. 2007. ISBN 9788755036413.

[17] Spendelow J, Babu P, Wieckowski A. Electrocatalytic oxidation of carbon monoxide and methanol on platinum surfaces decorated with ruthenium. Curr Opin Solid State Mater Sci 2005;9(12):37 – 48.

[18] Cao D, Lu GQ, Wieckowski a, Wasileski Sa, Neurock M. Mechanisms of methanol decomposition on platinum: A combined experimental and ab initio approach. The journal of physical chemistry B 2005;109(23):11622–33. doi:10.1021/jp0501188.

[19] Sriramulu S, Jarvi T, Stuve E. Reaction mechanism and dynamics of methanol electrooxidation on platinum(111). J Electroanal Chem (Lausanne Switz) 1999;467(1-2):132 –42.

[20] Iwasita T. Electrocatalysis of methanol oxidation. Electrochimica Acta 2002;47(2223):3663 –74. doi:10.1016/S0013-4686(02)00336-5.

[21] Lattner JR, Harold MP. Comparison of methanol-based fuel processors for pem fuel cell systems. Applied Catalysis B: Environmental 2005;56(12):149 –69. doi: 10.1016/j.apcatb.2004.06.024. ¡ce:title¿Fuel processing and PEM Fuel Cells: advanced cata;ysts, adsorbents and electrocatalysts¡/ce:title¿.

[22] Barsoukov E, Macdonald JR. Impedance Spectroscopy: Theory, Experiment, and Applications. Wiley - Interscience; 2nd edition ed.; 2005.

[23] Schmidt TJ, Baurmeister J. Properties of high-temperature PEFC Celtec-P 1000 MEAs in start/stop operation mode. Journal of Power Sources 2008;176(2):428–34. doi: 10.1016/j.jpowsour.2007.08.055.

[24] Li Q, Jensen JO, Savinell RF, Bjerrum NJ. High Temperature Proton Exchange Membranes Based on Polybenzimidazoles for Fuel Cells. Prog Polym Sci 2009;34(5):449 –77.

[25] Mamlouk M, Scott K. Analysis of high temperature polymer electrolyte membrane fuel cell electrodes using electrochemical impedance spectroscopy. Electrochim Acta 2011;56(16):5493 –512.

[26] Andreasen SJ, Vang JR, Kær SK. High temperature PEM fuel cell performance characterisation with CO and CO_2 using electrochemical impedance spectroscopy. Int J Hydrogen Energy 2011;36(16):9815 –30. European Fuel Cell 2009.

[27] Otomo J, Li X, Kobayashi T, Wen Cj, Nagamoto H, Takahashi H. AC-impedance spectroscopy of anodic reactions with adsorbed intermediates: electro-oxidations of 2-propanol and methanol on carbon-supported Pt catalyst. Journal of Electroanalytical Chemistry 2004;573(1):99–109. doi: 10.1016/j.jelechem.2004.07.002.

[28] Daletou MK, Kallitsis JK, Voyiatzis G, Neophytides SG. The Interaction of Water Vapors with H_3PO_4 Imbibed Electrolyte Based on PBI/polysulfone Copolymer Blends. J Memb Sci 2009;326(1):76 – 83.

[29] Liu G, Zhang H, Hu J, Zhai Y, Xu D, Shao Zg. Studies of performance degradation of a high temperature PEMFC based on H3PO4-doped PBI. Journal of Power Sources 2006;162(1):547–52. doi:10.1016/j.jpowsour.2006.07.008.

[30] Gu T, Shimpalee S, Zee JV, Chen CY, Lin CW. A study of water adsorption and desorption by a pbi-h3po4 membrane electrode assembly. Journal of Power Sources 2010;195(24):8194 –7. doi: 10.1016/j.jpowsour.2010.06.063.

[31] Zhang J, Zhang L, Bezerra CW, Li H, Xia Z, Zhang J, et al. EIS-assisted performance analysis of non-noble metal electrocatalyst (FeN/C)-based PEM fuel cells in the temperature range of 23-80C. Electrochim Acta 2009;54(6):1737 –43.

[32] Gomadam PM, Weidner JW. Analysis of electrochemi-

14

cal impedance spectroscopy in proton exchange membrane fuel cells. International Journal of Energy Research 2005;29(12):1133–51. doi:10.1002/er.1144.